Dipolar recoupling in solid state NMR by phase alternating pulse sequences

J. Lin [a], M.J. Bayro [b], R.G. Griffin [b], N. Khaneja [a,*]

[a] School of Engineering and Applied Sciences, Harvard University, Cambridge, MA 02138, USA
[b] Department of Chemistry and Francis Bitter Magnet Laboratory, Massachusetts Institute of Technology, Cambridge, MA 02139, USA

ARTICLE INFO

ABSTRACT

We describe some new developments in the methodology of making heteronuclear and homonuclear recoupling experiments in solid state NMR insensitive to rf-inhomogeneity by phase alternating the irradiation on the spin system every rotor period. By incorporating delays of half rotor periods in the pulse sequences, these phase alternating experiments can be made γ encoded. The proposed methodology is conceptually different from the standard methods of making recoupling experiments robust by the use of ramps and adiabatic pulses in the recoupling periods. We show how the concept of phase alternation can be incorporated in the design of homonuclear recoupling experiments that are both insensitive to chemical shift dispersion and rf-inhomogeneity.

1. Introduction

An important application of solid state nuclear magnetic resonance (NMR) spectroscopy is in structural analysis of "insoluble" protein structures such as membrane proteins, fibrils and extracellular matrix proteins which are exceedingly difficult to analyze using conventional atomic-resolution structure determination methods, including liquid state NMR and X-ray crystallography [1–5]. The goal of studying increasingly complex molecular systems is a strong motivation for the development of improved solid state NMR methods. The paper describes a set of new principles for design of heteronuclear and homonuclear dipolar recoupling experiments that are both broadband and insensitive of rf-field inhomogeneities. The merits of the proposed techniques with respect to state of the art methods is discussed.

For solids, the internal Hamiltonian not only contains isotropic interactions, such as isotropic chemical shifts and scalar J couplings, but also anisotropic (i.e., orientation dependent) chemical shifts and dipole–dipole coupling interactions in the case of coupled spin-1/2 nuclei. This implies that each molecule/crystallite in a "powder" sample may exhibit different nuclear spin interactions leading to severe line broadening and thereby reduced spectral resolution and sensitivity. This problem may be alleviated using magic-angle spinning (MAS), which averages these interactions and hereby results in high-resolution conditions for solid samples. However, this also results in loss of useful parts of the anisotropic interactions like dipolar couplings, which carry information about distances between nuclei and can help in obtaining

structural information. This has triggered the development of dipolar recoupling techniques [6,11–16], which selectively reintroduce these couplings to enable measurement of internuclear distances, torsion angles and transfer of magnetization from spin to spin in the molecule. Such recoupling experiments are the building blocks of essentially all biological solid state NMR experiments using "powder" samples. However, the recoupling experiments are sensitive to the amplitude of the radio-frequency fields and the orientation dependence of the dipolar coupling interaction.

The latter challenge motivates the present paper, where we present methods for making dipolar recoupling experiments insensitive to rf-inhomogeneity and Hartmann-Hahn mismatch by phase alternating the irradiation on the spins every rotor period. In [7], it was shown that this simple technique makes recoupling experiments less sensitive to the dispersion in the strength of the radio-frequency field. These experiments however do not achieve uniform transfer efficiency for all γ, where γ represents the rotation of the crystallite around the rotor axis. By introducing half rotor period delays in the middle of the proposed phase-alternating recoupling blocks, the recoupling is made insensitive to the angle γ. One standard technique for making recoupling experiments robust to Hartmann-Hahn mismatch is by using ramps or shaped adiabatic pulses [23,24] on the rf-power during the recoupling period. The described methodology is conceptually very different. The main contribution of this paper is the development of broadband homonuclear recoupling experiments that are robust to rf-inhomogeneity by using this concept of phase alternation. The main ideas described here are further developments of the recent work [25,26] on broadband homonuclear recoupling. We show that by using phase alternation, we can make experiments in [25,26], less sensitive to rf-inhomogeneity.

Phase alternating pulse sequences have appeared in solid state NMR experiments before [7–10]. The main contribution of this paper is further development of this methodology as a means to design robust recoupling experiments in various contexts.

2. Theory

Consider two coupled heteronuclear spins I and S under magic-angle spinning. The spins are irradiated with x phase rf-fields at their Larmor frequencies. In a double-rotating Zeeman frame, rotating with both the spins at their Larmor frequency, the Hamiltonian of the spin system takes the form

$$H(t) = \omega_I(t)I_z + \omega_S(t)S_z + \omega_{IS}(t)2I_zS_z + \omega_{rf}^I(t)I_x + \omega_{rf}^S(t)S_x, \quad (1)$$

where $\omega_I(t)$, $\omega_S(t)$ and $\omega_{IS}(t)$ represent time-varying chemical shifts for the two spins I and S and the coupling between them, respectively. These interactions may be expressed as a Fourier series

$$\omega_\lambda(t) = \sum_{m=-2}^{2} \omega_\lambda^m \exp(im\omega_r t), \quad (2)$$

where ω_r is the spinning frequency (in angular units) and $\tau_r = \frac{2\pi}{\omega_r}$ is the rotor period. The coefficients ω_λ $(\lambda = I, S, IS)$ reflect the dependence on the physical parameters like the isotropic chemical shift, anisotropic chemical shift, the dipole–dipole coupling constant and through this the internuclear distance [21]. $\omega_{rf}^I(t)$ and $\omega_{rf}^S(t)$ are the amplitudes of the rf-fields on spins I and S, respectively. If the rf-field strengths on the two spins is chosen to be integral (or half integral) multiples of the spinning frequency, i.e., $\omega_{rf}^I = p\omega_r$ and $\omega_{rf}^S = q\omega_r$, then the Hamiltonian for the dipole–dipole coupling in the interaction frame of the rf-irradiation averages over a rotor period to

$$\overline{H} = \frac{1}{4}\{(\omega_{IS}^{-(p+q)} + \omega_{IS}^{(p+q)})(2I_zS_z - 2I_yS_y) + (\omega_{IS}^{-(p-q)} + \omega_{IS}^{(p-q)})$$
$$\times (2I_zS_z + 2I_yS_y) - i(\omega_{IS}^{-(p+q)} - \omega_{IS}^{(p+q)})(2I_zS_y$$
$$+ 2I_yS_z)i(\omega_{IS}^{-(p-q)} - \omega_{IS}^{(p-q)})(2I_zS_y - 2I_yS_z)\}. \quad (3)$$

Choosing $p - q = -1$ and $|p + q| > 2$, we prepare the effective Hamiltonian,

$$H_{dcp}(\gamma) = \kappa\{\cos(\gamma)(I_zS_z + I_yS_y) - \sin(\gamma)(I_zS_y - I_yS_z)\}, \quad (4)$$

where γ as before is the Euler angle discriminating the crystallites by rotation around the rotor axis. This is the standard DCP experiment [6]. The scaling factor

$$\kappa = \frac{1}{2\sqrt{2}}b_{IS}\sin(2\beta), \quad (5)$$

depends on the dipole–dipole coupling constant b_{IS} and the angle β between the internuclear axis and the rotor axis.

2.1. MOIST experiment

The effective Hamiltonian H_{dcp} mediates the coherence transfer $I_x \to S_x$ with an efficiency independent of the γ Euler angle. This transfer experiment is however sensitive to rf-inhomogeneity as described below. We consider rf-inhomogeneity on the two channels, such that rf-amplitude on the I channel is $\omega_{rf}^I = p(1 + \epsilon_I)\omega_r$ and rf-amplitude on the S channel is $\omega_{rf}^S = q(1 + \epsilon_S)\omega_r$. Here ϵ_I and ϵ_S represent the rf-inhomogeneity on the two channels I and S, respectively.

In the interaction frame of the rf-irradiation, with nominal rf-strength $p\omega_r$ and $q\omega_r$, the natural Hamiltonian of the spin system averages to

$$\tilde{H}(\gamma) = H_{dcp}(\gamma) + \epsilon^- \omega_r \frac{I_x - S_x}{2} + \epsilon^+ \omega_r \frac{I_x + S_x}{2}, \quad (6)$$

where $\epsilon^- = p\epsilon_I - q\epsilon_S$ and $\epsilon^+ = p\epsilon_I + q\epsilon_S$. Let operators X^-, Y^- and Z^- represent the zero quantum operators $\frac{I_x - S_x}{2}$, $I_zS_z + I_yS_y$ and $I_zS_y - I_yS_z$, respectively. Similarly, X^+, Y^+ and Z^+ represent the double quantum operators $\frac{I_x + S_x}{2}$, $I_zS_z - I_yS_y$ and $I_zS_y + I_yS_z$, respectively. The DCP Hamiltonian in Eq. (4) inverts the operator X^- in the zero quantum frame as depicted by the trajectory A in Fig. 1. In the presence of the Hartmann-Hahn mismatch, measured by the parameter ϵ^-, the operator X^- executes a rotation around the tilted axis leading to poor inversion, as depicted by trajectory B in Fig. 1.

Fig. 2A shows the efficiency η of $^{15}N \to ^{13}C$, coherence transfer for the DCP experiment as a function of the mixing time τ_d. The build up curve is shown for different (increasing) values of ϵ^-. Observe that even for a small mismatch, corresponding to $\epsilon^- = .01$, (1% of the rotor frequency), the efficiency of coherence transfer is significantly reduced. This sensitivity to mismatch can be significantly reduced by introducing the concept of phase-alternating pulse sequences.

We now describe the concept of phase-alternating pulse sequences as introduced in [7] for compensating rf-inhomogeneity in the system. Consider the pulse sequence in Fig. 3A, where the phase on both I and S channel is changed between $+x$ and $-x$ every rotor period. In [7], this experiment is called MOIST. To analyze the effect of this pulse sequence, in Eq. (6), we can omit the operator X^+, as it commutes with all operators in the zero quantum frame. In the interaction frame of the rf-field, the effective Hamiltonian in the first rotor period is

$$H_1 = H_{dcp}(\gamma) + \epsilon^- \omega_r X^-, \quad (7)$$

and the effective Hamiltonian in the second rotor period is

$$H_2 = H_{dcp}(-\gamma) - \epsilon^- \omega_r X^-. \quad (8)$$

The effective Hamiltonian from the phase alternation is

$$\frac{H_1 + H_2}{2} \sim \frac{\kappa}{2}\cos(\gamma)(I_zS_z + I_yS_y),$$

where we have used the small flip angle approximation ($\kappa\tau_r \ll 1$) and assumed that

$$\exp(-iH_1\tau_r)\exp(-iH_2\tau_r) \sim \exp(-i(H_1 + H_2)\tau_r).$$

This Hamiltonian is not γ encoded. The resulting efficiency of transfer is lower as compared to the γ encoded experiments. Fig. 2B shows the transfer efficiency as a function of the mixing
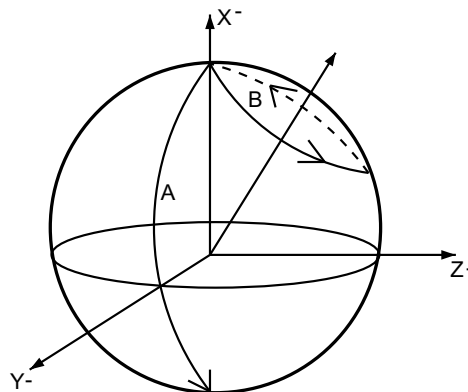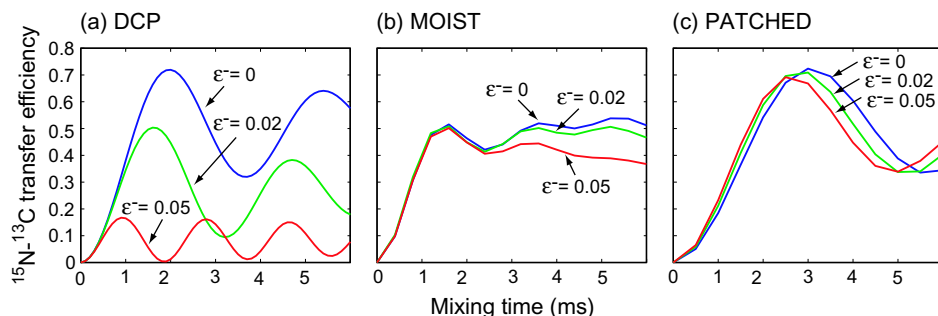

Fig. 1. The figure depicts the zero quantum frame, where the transfer $I_x \to S_x$ is simply viewed as the inversion of the initial operator $X^- \to -X^-$. In the presence of rf-inhomogeneity, the inversion is incomplete, as the rotation X^- is performed around the tilted axis as shown in the above figure.

Fig. 2. The above three panels show efficiency η of $^{15}\text{N} \rightarrow {}^{13}\text{C}$, coherence transfer for the DCP, MOIST and PATCHED experiment as a function of the mixing time τ_d, with experimental conditions corresponding to MAS experiments with 10 kHz spinning and using a 360 MHz (Larmor frequency of ^1H) magnet. The nominal rf-field strength of $\omega_{rf}^C/2\pi = 50$ kHz and $\omega_{rf}^N/2\pi = 40$ kHz were used. The calculations used $\delta_{iso}^C = 0$, $\delta_{aniso}^C = 19.43$ ppm, $\eta^C = .98$, $\{\alpha_{PR}^C, \beta_{PR}^C, \gamma_{PR}^C\} = \{64.9°, 37.3°, -28.8°\}$, $\delta_{iso}^N = 10$, $\delta_{aniso}^N = 10.1$ ppm, $\eta^N = .17$, $\{\alpha_{PR}^N, \beta_{PR}^N, \gamma_{PR}^N\} = \{-83.8°, -79.0°, 0.0°\}$ and internuclear distance $r_{CN} = 1.52$ A°, $\{\alpha_{PR}^{CN}, \beta_{PR}^{CN}, \gamma_{PR}^{CN}\} = \{0°, 0°, 0°\}$ and $J_{CN} = -11$ Hz. The rf-power of $\omega_{rf}^N/2\pi = 40$ kHz, on the nitrogen channel is now changed from the nominal value to $40(1 + \epsilon^-)$kHz. The build up curve for different values of epsilon (expressed in %) are plotted. The top left panel is the standard DCP experiment. The top right experiment is the phase alternating DCP experiment as shown in Fig. 3B, which is not γ encoded. The bottom panel shows the phase alternating DCP experiment which is γ encoded as shown in Fig. 3C. rf-Power of $\omega_{rf}^N/2\pi = \omega_{rf}^C/2\pi = 60$ kHz is used on both the channels during the half rotor period delays of $\frac{\tau_r}{2}$ to eliminate chemical shift evolution.
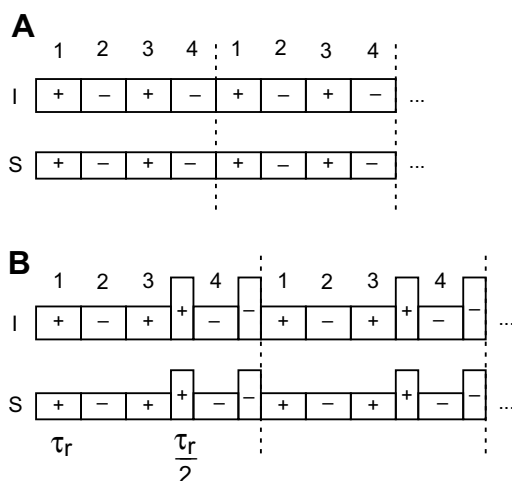
Fig. 3. In (A) is shown the basic idea of the MOIST experiment, where the phase of the rf-field is switched every τ_r units of time. In (B) is shown the PATCHED experiment, where introducing delays of $\frac{\tau_r}{2}$, preceding and past every fourth period keeps the γ encoding property of the recoupled Hamiltonian. The rf-power on both channels during half rotor period delays is chosen to avoid Hartmann–Hahn matching and rotary resonance and prevent dipolar recoupling.

time for the phase alternating pulse sequence for different degrees of rf-inhomogeneity. Comparison to Fig. 2A shows that this sequence is more robust to rf-inhomogeneity.

2.2. PATCHED experiment

We now present a method to make this phase alternating pulse sequence γ encoded. We call this experiment PATCHED (*P*hase *A*lternating experiment *C*ompensated by *H*alf rotor p*E*riod *D*elays). Fig. 3B shows the pulse sequence, consisting of a five rotor period building block, which is subsequently repeated many times, depending on the desired mixing period.

In the interaction frame of the nominal rf-irradiation, the first and third rotor period prepares the same effective Hamiltonian H_1 as in Eq. (7). The second rotor period prepares the same effective Hamiltonian H_2 as in Eq. (8). Following the third rotor period, a half rotor period delay moves the crystallites with angle γ to $\gamma + \pi$. In the final recoupling period, one prepares the effective Hamiltonian,

$$H_4 = H_{dcp}(-(\gamma + \pi)) - \epsilon^- \omega_r X^-. \tag{9}$$

Again, using the small angle approximation, we sum up the four Hamiltonians to get the effective Hamiltonian $\overline{H}$, such that

$$4\overline{H} = (H_{dcp}(\gamma) + \epsilon^- \omega_r X^-) + (H_{dcp}(-\gamma) - \epsilon^- \omega_r X^-) + (H_{dcp}(\gamma) + \epsilon^- \omega_r X^-) + (H_{dcp}(-\gamma - \pi) + \epsilon^- \omega_r X^-).$$

The resulting effective Hamiltonian $\overline{H}$ to leading order is then

$$\overline{H} = \frac{2\kappa}{5} \{\cos(\gamma)(I_z S_z + I_y S_y) - \sin(\gamma)(I_z S_y - I_y S_z)\}.$$

This is a γ encoded Hamiltonian, simply scaled down by a factor of $\frac{2}{5}$. To leading order, the effect of inhomogeneous rf-field gets canceled. Fig. 2B and C shows the transfer efficiency as a function of the mixing time for the presented phase-alternating and γ encoded phase alternating pulse sequence for different rf-inhomogeneity. The sequence achieves the same transfer efficiency as the γ encoded pulse sequences and are robust to rf-inhomogeneity.

Fig. 4 shows the experimental results comparing transfer efficiency as a function of rf-mismatch of the three experiments DCP, MOIST and PATCHED experiment.

3. Homonuclear spins

The methods presented in the previous section generalize in a straightforward way to homonuclear spins. To fix ideas, we begin by considering two homonuclear spins I and S under magic-angle spinning condition. A classical technique for recoupling the spins is the HORROR experiment [13]. The spins are irradiated with an rf-field strength of $\frac{\omega_r}{2}$, where ω_r is the rotor frequency. In a rotating frame, rotating with both the spins at their Larmor frequency, the Hamiltonian of the spin system takes the form

$$H(t) = \omega_I(t)I_z + \omega_S(t)S_z + \omega_{IS}(t)(3I_z S_z - I \cdot S) + \frac{\omega_r}{2}F_x, \tag{10}$$

where the operator $F_x = I_x + S_x$, and $\omega_I(t)$ and $\omega_S(t)$ represent the chemical shift for the spins I and S, respectively, and $\omega_{IS}(t)$ represents the time varying couplings between the spins under magic-angle spinning. The chemical shifts and the time varying couplings can be expressed using Fourier series as in Eq. (2).

The term $I \cdot S$ in Eq. (10), commutes with the rf-Hamiltonian, $\frac{\omega_r}{2}F_x$, as it averages under MAS. We will, therefore, drop this term in the subsequent treatment. In the interaction frame of the rf-irradiation, the internal Hamiltonian from Eq. (1), takes the form

$$H_I(t) = \frac{3}{2}\omega_{IS}(t)Z^- + \frac{3}{2}\omega_{IS}(t)(Z^+ \cos(\omega_r t) + Y^+ \sin(\omega_r t)), \tag{11}$$
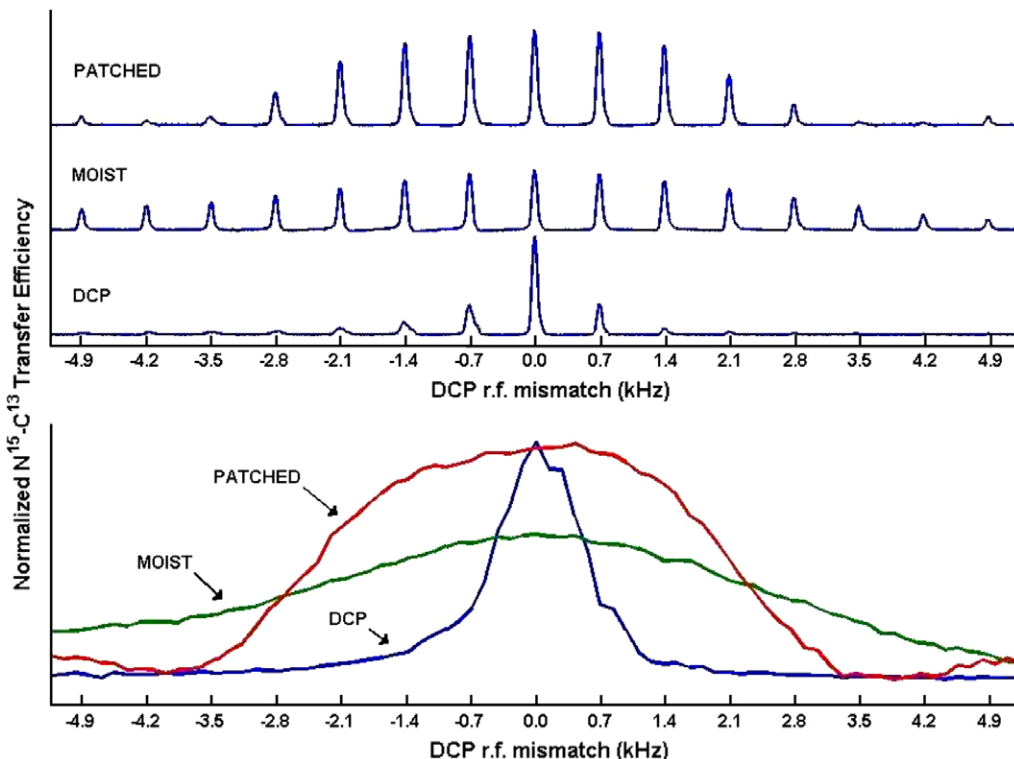
Fig. 4. The above figure shows the experimental spectra for DCP, Phase-alt (MOIST) and PATCHED experiments for $^{15}N \rightarrow ^{13}C_\alpha$, transfer for a powder $^{13}C_\alpha$, ^{15}N labeled glycine using MAS spinning at $\frac{\omega_r}{2\pi} = 8$ kHz and CW decoupling on protons of $\frac{\omega_{rf}^H}{2\pi} = 100$ kHz. The nominal power on $^{13}C_\alpha$ and ^{15}N was calibrated to be $\frac{\omega_{rf}^C}{2\pi} = 22.2$ kHz and $\frac{\omega_{rf}^N}{2\pi} = 30.2$ kHz. The bottom panel shows the transfer profile when the carbon power is varied from its nominal value. The top panel shows sample spectra from the transfer profile in the bottom panel for discrete values of the $\frac{\omega_{rf}^C}{2\pi}$ around the nominal value. The nominal power on $^{13}C_\alpha$ and ^{15}N during the half rotor period delays was calibrated to be $\frac{\omega_{rf}^C}{2\pi} = 22.2$ kHz and $\frac{\omega_{rf}^N}{2\pi} = 20.2$ kHz.

where, X^-, Y^-, Z^- are zero quantum operators and X^+, Y^+, Z^+ are multiple quantum operators as defined before. To begin, we assume that $\omega_I(t)$ and $\omega_S(t)$ are significantly smaller than the rf-power $\frac{\omega_r}{2}$ and therefore, they average out in the interaction frame of the rf-irradiation. The modulation $\cos \omega_r t$, caused by the rf-field, generates a secular term with the modulation due to the MAS. This results in the effective γ encoded Hamiltonian,

$$H_{\text{hom}}(\gamma) = \kappa_h[\cos(\gamma)(I_zS_z - I_yS_y) - \sin(\gamma)(I_zS_y + I_yS_z)], \quad (12)$$

where the scaling factor

$$\kappa_h = \frac{3}{4\sqrt{2}} b_{IS} \sin(2\beta) \quad (13)$$

depends on the dipole–dipole coupling constant b_{IS}. In the multiple quantum frame spanned by the operators $\{X^+, Y^+, Z^+\}$, the effective Hamiltonian $H_{\text{hom}}(\gamma)$ inverts the initial operator $X^+ \rightarrow -X^+$ and transfers the initial state $I_x \rightarrow S_x$.

3.1. Broadband homonuclear recoupling

In practice, $\omega_I(t)$ and $\omega_S(t)$ may be comparable or larger than ω_r, and therefore the proposed methodology is narrowband and gives poor transfer efficiency in the presence of Larmor dispersion. Subsequently, we will address the problem of making these homonuclear sequences broadband. We first show how the concept of phase alternating pulse sequences can be applied to the present context.

The inhomogeneity is modeled by a parameter ϵ, such that the rf-Hamiltonian of the system takes the form

$$H^{\text{rf}} = \frac{\omega_r}{2}(1 + \epsilon)F_x. \quad (14)$$

In the interaction frame of rf-irradiation along x axis, with strength $\frac{\omega_r}{2}$, the Hamiltonian of the system in (10) averages to

$$H_I = H_{\text{hom}}(\gamma) + \epsilon \frac{\omega_r}{2} F_x. \quad (15)$$

The Hamiltonian gives a poor transfer of the initial operator $X^+ \rightarrow -X^+$, (and therefore also for the transfer of state $I_x \rightarrow S_x$) when $\epsilon \omega_r \sim \kappa$, where κ is as in Eq. (12). As seen in Fig. 6A, an ϵ value of .05, will lead to appreciable loss in the transfer efficiency.

Analogous to experiments in Fig. 3A and C, are the homonuclear recoupling experiments shown in Fig. 5A and B. The experiment in Fig. 5B is phase alternating, γ encoded version of the experiment in Fig. 5A. The analysis of these phase alternating homonuclear exper-
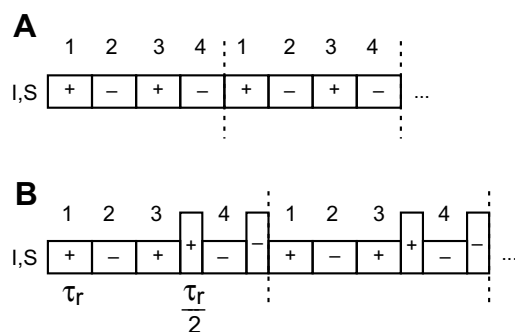
Fig. 5. In (A) is shown the phase alternating HORROR experiment, where the phase of the rf-field is switched every τ_r units of time. In (B) is shown a modified version of the sequence in (A), where introducing delays of $\frac{\tau_r}{2}$, preceding and past every fourth period keeps the γ encoding property of the recoupled Hamiltonian.

iments is very similar to their heteronuclear counterparts. For sake of completion, we present the analysis here.

In Fig. 5B, in the interaction frame of the x-phase rf-irradiation with strength $\frac{\omega_r}{2}$, in the first and third rotor period, we prepare the effective Hamiltonian,

$$H_1 = H_3 = H_{\text{hom}}(\gamma) + \frac{\epsilon \omega_r}{2} F_x. \tag{16}$$

In the second rotor period, an effective Hamiltonian

$$H_2 = H_{\text{hom}}(-\gamma) - \frac{\epsilon \omega_r}{2} F_x, \tag{17}$$

is prepared.

In the fourth recoupling period (following the half rotor period delay), the effective Hamiltonian,

$$H_4 = H_{\text{hom}}(-\gamma - \pi) - \frac{\epsilon \omega_r}{2} F_x, \tag{18}$$

is produced. The net Hamiltonian, to leading order, is then

$$\overline{H} = \frac{H_1 + H_2 + H_3 + H_4}{4}$$
$$= \frac{2\kappa}{5} \{\cos(\gamma)(I_z S_z - I_y S_y) + \sin(\gamma)(I_z S_y + I_y S_z)\}. \tag{19}$$

Observe, to leading order, the inhomogeneity in the field gets canceled by phase alternation. The recoupling Hamiltonian is scaled down by a factor of $\frac{2}{5}$, compared to standard HORROR experiment. Fig. 6A, shows the transfer efficiency vs mixing time curves for the HORROR experiment shown in the Fig. 5A with different levels of rf-inhomogeneity. Fig. 6B shows the transfer efficiency
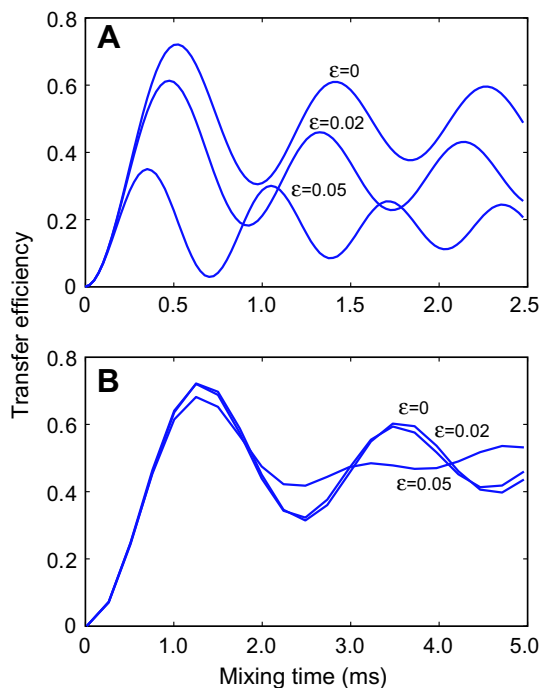
Fig. 6. In (A) is shown the transfer efficiency vs mixing time curves for the HORROR experiment (Fig. 5A) with different level of rf-inhomogeneity. Numerical simulation are performed for an on resonance, ^{13}C–^{13}C spin-pair, 1.52 Å apart in a powder sample subject to 20 kHz MAS, an external magnetic field corresponding to a 360 MHz (Larmor frequency for ^{1}H) spectrometer, and nominal rf-field strength on the ^{13}C channel of 10 kHz. In (B) is shown the transfer efficiency vs mixing time curves for the phase alternating HORROR experiment Fig. 5B. rf-Power of $\omega_{\text{rf}}^C/2\pi = 40$ kHz is used during the half rotor period delays of $\frac{\tau_r}{2}$ to prevent chemical shift evolution and recoupling.

vs mixing time curves for the phase alternating HORROR experiment shown in Fig. 5B. Note, both experiments in Fig. 5A and B are narrowband and work in the regime $\omega_r \gg \omega_I(t), \omega_S(t)$.

In practice, $\omega_I(t)$ and $\omega_S(t)$ may be comparable or larger than ω_r and therefore, the proposed methodology gives poor transfer efficiency in the presence of large Larmor dispersions. We now address the problem of making these homonuclear sequences broadband by a suitable modulation of the rf-field as described below. The main ideas presented here are further developments on the recent work [25,26] on broadband homonuclear recoupling. The homonuclear recoupling experiments presented [25,26] are sensitive to rf-inhomogeneity. We now show how the concept of phase alternation can be incorporated to make these experiments immune to rf-inhomogeneity.

Consider the rf-irradiation on homonuclear spin-pair whose amplitude is chosen as $A(t) = \frac{C}{2\pi}$ and the offset $\Delta\omega(t) = \omega_r \sin(Ct)$. This offset is implemented as a phase modulation

$$\phi(t) = \frac{2\omega_r}{C} \sin^2(Ct) = \frac{\omega_r}{C}(1 - \cos(Ct))$$

so that the rf-Hamiltonian, takes the form

$$H^{\text{rf}}(t) = CF_x - \omega_r \sin(Ct)F_z, \tag{20}$$

where C is in angular frequency units and we choose $C \gg \omega_I(t), \omega_S(t), \omega_r$. In the interaction frame of the irradiation along x axis, with the strength C, the coupling Hamiltonian of the spin system takes the form

$$H_I^{\text{DD}}(t) = \frac{3}{2}\omega_{IS}(t)(I_z S_z + I_y S_y) + \frac{3}{2}\omega_{IS}(t)((I_z S_z - I_y S_y)\cos Ct$$
$$+ (I_z S_y + I_y S_z)\sin Ct), \tag{21}$$

and the rf-Hamiltonian of the spin system transforms to

$$H_I^{\text{rf}}(t) = \frac{\omega_r}{2}(-\cos 2Ct\, F_z + 2\sin^2 Ct F_y), \tag{22}$$

which averages over a period $\tau_c = 2\pi/C$ to

$$H_I^{\text{rf}} = \frac{\omega_r}{2}F_y. \tag{23}$$

Now, transforming into the interaction frame of the rf-Hamiltonian H_I^{rf}, we only retain terms that give secular contributions to the effective Hamiltonian, i.e., terms oscillating with frequency C are dropped and the residual Hamiltonian takes the form

$$H_{II}(t) = \kappa_h\{\cos(\omega_r t)\cos(\omega_r t + \gamma)(I_z S_z - I_x S_x) + \sin(\omega_r t)$$
$$\times \cos(\omega_r t + \gamma)(I_z S_x + I_x S_z)\}, \tag{24}$$

which over a rotor period averages to

$$\overline{H}_{II} = \frac{\kappa_h}{2}\{\cos(\gamma)(I_z S_z - I_x S_x) - \sin(\gamma)(I_z S_x + I_x S_z)\}, \tag{25}$$

where κ_h is as in Eq. (12). The Hamiltonian $\overline{H}_{II}$ performs the transfer $I_y \leftrightarrow S_y$.

This cosine modulated pulse sequence is broadband as a large value of C averages out the chemical shift [25,26]. The main drawback of the high power cosine modulated pulse sequence is its sensitivity to rf-inhomogeneity. To analyze the effect of inhomogeneity, let ϵ denote the inhomogeneity parameter. Then, rewriting H_{rf} in Eq. (20) gives

$$H^{\text{rf}}(t) = C(1 + \epsilon)F_x - \omega_r \sin(Ct)F_z. \tag{26}$$

In the interaction frame of irradiation along x axis with strength C, the rf-Hamiltonian averages to $\epsilon C F_x + \frac{\omega_r}{2} F_y$. Now, proceeding to the interaction frame of the rf-Hamiltonian $\frac{\omega_r}{2}F_y$, the dipolar Hamiltonian of the spin system averages to

$$H_{\text{eff}} = \overline{H}_{II}, \tag{27}$$

where $\overline{H}_{II}$ is as in the Eq. (25). In this interaction frame, the Hamiltonian $\overline{H}_{II}$ performs the dipolar recoupling. However, for large C, the factor ϵCF_x may significantly reduce the HORROR matching condition.

3.2. PAMORE experiment

Here, we present a method to eliminate this effect of the rf-inhomogeneity by simply phase alternating every $\tau_c = \frac{2\pi}{C}$ units of time, by making $\phi(t + \tau_c) = \pi - \phi(t)$. We call this pulse sequence PAMORE (*P*hase *A*lternating *MO*dulated *RE*coupling). This results in switching the rf-Hamiltonian every τ_c units of time between

$$H_1^{\text{rf}}(t) = (1 + \epsilon)CF_x - \omega_r \sin(Ct)F_z; H_2^{\text{rf}}(t)$$
$$= -(1 + \epsilon)CF_x + \omega_r \sin(Ct)F_z. \tag{28}$$

The top panels in Fig. 7 show the phase modulation of the rf-field over a rotor period for the CMRR and PAMORE pulse sequences, respectively.

To analyze the effect of the pulse sequence, whereby the rf-Hamiltonian is switched between $H_1^{\text{rf}}(t)$ and $H_2^{\text{rf}}(t)$, let us first transform into the interaction frame of the Hamiltonian that switches between CF_x and $-CF_x$, every τ_c units of time.

Therefore, in the first τ_c, one obtains an effective rf-Hamiltonian,

$$H_1^{\text{rf}} = \epsilon CF_x + \frac{\omega_r}{2}F_y, \tag{29}$$

followed by the Hamiltonian

$$H_2^{\text{rf}} = -\epsilon CF_x + \frac{\omega_r}{2}F_y. \tag{30}$$

The effective rf-Hamiltonian one prepares is

$$\overline{H}^{\text{rf}} = \frac{H_{\text{rf}}^1 + H_{\text{rf}}^2}{2} = \frac{\omega_r}{2}F_y. \tag{31}$$

If C is chosen large enough, the coupling Hamiltonian $H_I^{\text{DD}}(t)$, in the interaction frame takes the form, $\frac{3\omega_{IS}(t)}{2}(I_zS_z + I_yS_y)$, where fast oscillating component at frequency C have been neglected, as they average out. Now, proceeding to the interaction frame of the rf-Hamiltonian in Eq. (31), the total Hamiltonian of the spin system averages to $\overline{H}_{II}$ as in the Eq. (25). To leading order, the effect of inhomogeneity is canceled out.

Fig. 7 shows simulations comparing the homonuclear recoupling transfer efficiency obtained using CMRR and PAMORE pulse sequence for three different values of ϵ (0, .02, .05).

The PAMORE pulse sequence can be further compensated against dispersion in the angle β by adiabatically changing the amplitude of the sinusoidally varying offset, i.e,

$$\phi(t) = m(t)\pi + (-1)^{m(t)}\frac{a(t)}{C}(1 - \cos Ct),$$

where $m(t)$ switches between 0 and 1 every t_c period. This modulation of the phase is depicted in Fig. 7II. This modulation then corresponds to switching between Hamiltonians

$$H^{\text{rf}}(\pm) = \pm\{(1 + \epsilon)CF_x \pm a(t)\sin(Ct)F_z\}, \tag{32}$$

where $a(t)$ is a shaped pulse as described below.

We transform into the interaction frame of the Hamiltonian that switches between CF_x and $-CF_x$, every τ_c units of time. Analogous to Eq. (31), the effective Hamiltonian we prepare over two rotor periods is then
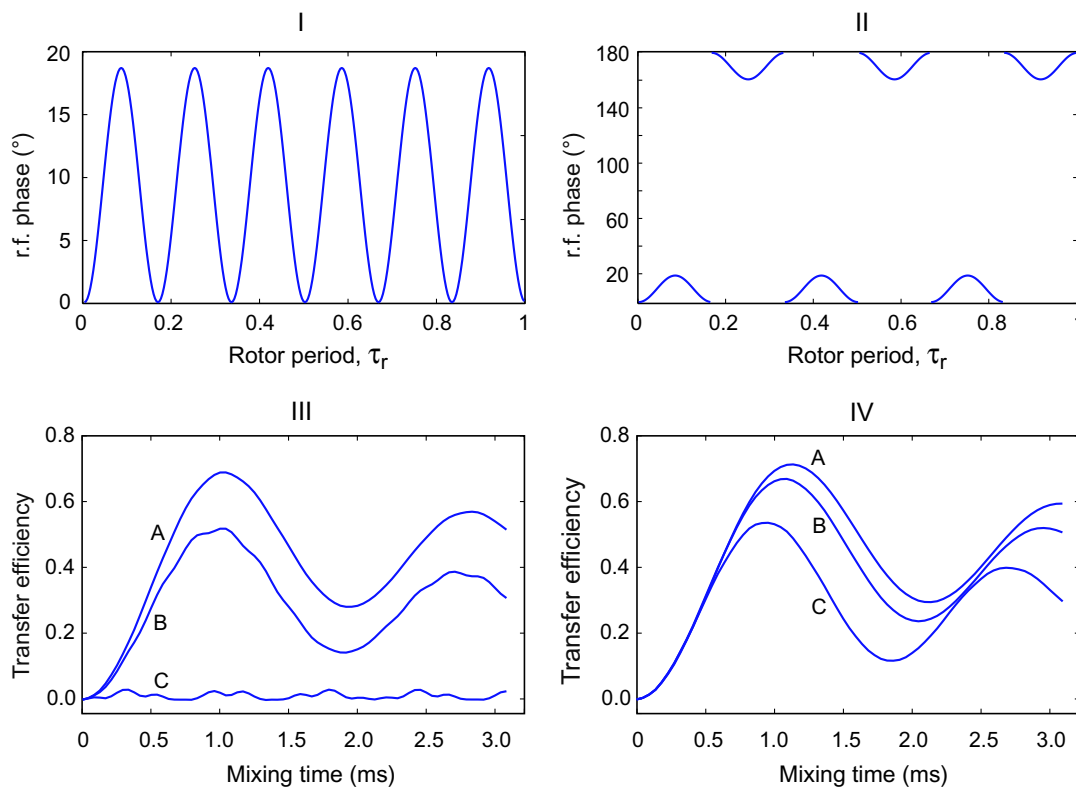
Fig. 7. The top two panels show the phase of the rf-irradiation as a function of time (in the units of τ_r) for the CMRR (I) and PAMORE (II) pulse sequences when $C = 6\omega_r$. The bottom two panel show numerical simulations of the transfer efficiency for the ^{13}C–^{13}C spin-pair, 1.52 Å apart in a powder sample subject to 8 kHz MAS, an external magnetic field corresponding to a 360 MHz (Larmor frequency for ^{1}H) spectrometer and nominal rf-field strength on the ^{13}C channel of 48 kHz, for the CMRR (III) and PAMORE (IV) pulse sequences, for three different values of ϵ (0, .02, .05) shown as curves A, B and C. Simulations use $C = 6\omega_r$, giving $\tau_c = 125/6$ μs and rf-power of $\omega_{\text{rf}}^C/2\pi = 48$ kHz. The efficiency falls down with increasing ϵ. In panel III at $\epsilon = .05$, there is almost no transfer.

$$\overline{\mathscr{H}}^{\text{rf}} = \frac{a(t)}{2}F_y, \tag{33}$$

and the effective Hamiltonian is

$$\overline{\mathscr{H}}^{\text{eff}} = \frac{3}{2}\omega_{IS}(t)(I_zS_z + I_yS_y) + \frac{a(t)}{2}F_y. \tag{34}$$

Now, as $a(t)$ is swept adiabatically (or ramped) from $\omega_r - \Delta$ to $\omega_r + \Delta$, the operator X^+ is inverted to $-X^+$, over the broader range of values of β. This is the standard principle of adiabatic following that guides design of ramped or adiabatic pulses.

4. Results

All experiments were performed on a 360 MHz spectrometer ([1]H Larmor frequency of 360 MHz) equipped with a triple resonance 4 mm probe. The data from uniformly ^{13}C, [15]N -labeled samples of glycine (purchased from Cambridge Isotope Laboratories, Andover, MA) was obtained using the full volume of standard 4 mm rotor at ambient temperature using $\frac{\omega_r}{2\pi} = 8$ kHz sample spinning. The experiments used 3 s recycling delay, 8 scans, ^{1}H to ^{15}N cross-polarization with rf-field strength of 54 (^{1}H) and 58–68 (^{15}N ramped) kHz, respectively, and duration 1.5 ms.

Fig. 4 shows the experimental ^{13}C spectra for DCP, Phase-alt (MOIST) and PATCHED experiments for the [15]N → [13]C$_\alpha$, following the ^{1}H to ^{15}N cross-polarization. The experiment used CW decoupling on protons of $\frac{\omega_{\text{rf}}^H}{2\pi} = 100$ kHz during the transfer. The nominal power on [13]C$_\alpha$ and ^{15}N was calibrated to be $\frac{\omega_{\text{rf}}^C}{2\pi} = 22.2$ kHz and $\frac{\omega_{\text{rf}}^N}{2\pi} = 30.2$ kHz to optimize the transfer efficiency of the DCP experiment. The bottom panel in Fig. 4 shows the transfer profile for the DCP, MOIST and PATCHED experiments, when the carbon power is varied from its nominal value. The top panel shows sample spectra from the transfer profile in the bottom panel for discrete values of the $\frac{\omega_{\text{rf}}^C}{2\pi}$ around the nominal value. The nominal power on [13]C$_\alpha$ and ^{15}N during the half rotor period delays was calibrated to be $\frac{\omega_{\text{rf}}^C}{2\pi} = 22.2$ kHz and $\frac{\omega_{\text{rf}}^N}{2\pi} = 20.2$ kHz, respectively. The powers are chosen large enough to prevent chemical shift evolution and avoid Hartmann-Hahn and rotary resonance conditions and thereby prevent dipolar recoupling. The exact values are experimentally optimized.

As expected from theory and simulations, the MOIST experiment is much more robust to rf-inhomogeneity compared to the standard DCP experiment. However, it is not a γ encoded experiment and therefore has a lower transfer efficiency. The PATCHED experiment is both insensitive to rf-inhomogeneity and γ encoded as seen from Fig. 4.

Fig. 8, shows the experimental spectra for CMRR and PAMORE pulse sequences, for the [13]C$_\alpha$ → [13]CO transfer following the ^{1}H to ^{15}N CP transfer and ^{15}N to [13]C$_\alpha$ DCP transfer. The CP and DCP steps used the same rf-powers as calibrated in experiment 1 in Fig. 4. CW decoupling on protons of $\frac{\omega_{\text{rf}}^H}{2\pi} = 100$ kHz was used during the experiment. The nominal power on ^{13}C channel during the CMRR and PAMORE experiment was calibrated to $\frac{\omega_{\text{rf}}^C}{2\pi} = 48$ kHz with the carrier placed midway between C$_\alpha$ and CO resonances that are 12 kHz apart. The rf-power is chosen sufficiently large to prevent ^{13}C chemical shift evolution and make the recoupling broadband. In principle, sufficiently large power on carbon should also decouple protons. However, we use conventional CW decoupling on protons of $\frac{\omega_{\text{rf}}^H}{2\pi} = 100$ kHz and therefore moderate rf-power is used on ^{13}C channel for effective decoupling. The phase modulation over one rotor period for the CMRR and PAMORE pulse sequence are shown in panels I and II in Fig. 7. Both experiments used 15 rotor periods for the full transfer and start with initial y magnetization on [13]C$_\alpha$ following [15]N → [13]C$_\alpha$ DCP transfer.

It is evident from the simulation results in Fig. 7 and the experimental data in Fig. 8 that the PAMORE experiment is significantly less sensitive to rf-inhomogeneity. Here we have used modest rf-power of 48 kHz on the ^{13}C channel to make the Homonuclear recoupling broadband. This however requires separate proton decoupling. By simply increasing the power on the carbon channel, we can eliminate the need for proton decoupling as the same rf-field on carbon can help to decouple protons. This has been suggested as a merit of the CMRR like pulse sequences as it can significantly reduce sample heating [25,26]. However, the issue of sensitivity to rf-inhomogeneity becomes even more critical as we use more rf-power on the carbon as argued in Eq. (27). Therefore, the use of PAMORE pulse elements becomes even more useful at high ^{13}C powers.

5. Conclusion

In this article, we reported some new developments based on the concept of phase alternating pulse sequences for the design of heteronuclear and homonuclear recoupling experiments that are insensitive to rf-inhomogeneity. The principle was finally applied to the development of improved homonuclear recoupling experiments.

The techniques presented here can be incorporated in more elaborate experiment design that can also compensate for the dispersion in the angle β in Eqs. (5) and (13). In our recent work [17], we showed the analogy between the problem of dipolar recoupling in the presence of anisotropies in β and the strength of rf-field to a problem of control of single spin in the presence of rf-inhomogeneity and Larmor dispersion, respectively. Using this analogy, we demonstrated how ideas of composite pulse sequences [18–20] from liquid state NMR can be incorporated in dipolar recoupling experiments to make them insensitive to angle β and rf-inhomogeneity. It is now possible to construct a family of dipolar recoupling experiments of increasing length and degree of compensation that
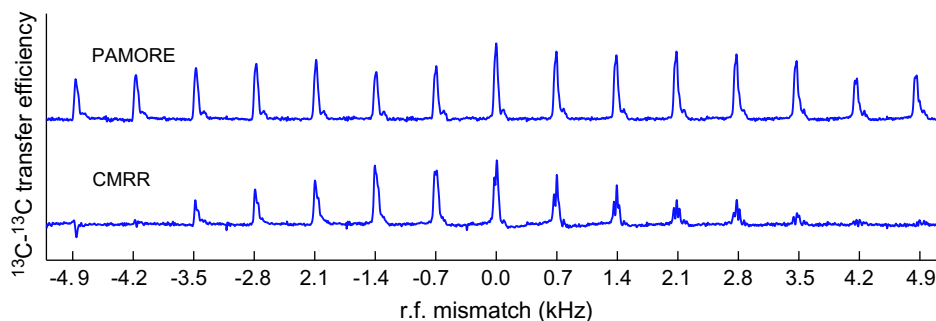
Fig. 8. The top panel shows the experimental spectra for CMRR and PAMORE pulse sequences, [13]C$_\alpha$ → [13]CO, transfers for a powder ^{13}C, ^{15}N labeled glycine using MAS spinning at $\frac{\omega_r}{2\pi} = 8$ kHz and CW decoupling on protons of $\frac{\omega_{\text{rf}}^H}{2\pi} = 100$ kHz. The nominal power on ^{13}C channel was calibrated to 48 kHz with the carrier placed midway between C$_\alpha$ and CO resonances that are 12 kHz apart. The phase modulation over one rotor period for the CMRR and PAMORE pulse sequence are shown in panels I and II in Fig. 7. Both experiments used 15 rotor periods for the full transfer and start with initial y magnetization on [13]C$_\alpha$ following [15]N → [13]C$_\alpha$ DCP transfer.

ultimately achieve 100% transfer efficiency for all orientations of the dipolar coupling tensor. However, these composite pulse sequences tend to be long, especially in the presence of rf-inhomogeneity which translates into large Larmor dispersion in the single spin picture. Therefore, elaborate designs are needed to compensate for this rf-inhomogeneity. Based on the methods presented in this paper, significantly shorter composite recoupling pulse sequences can be engineered based on phase alternating recoupling blocks. This essentially reduces the problem to compensating only for dispersion in angle β, which takes significantly shorter composite dipolar recoupling experiments.

Furthermore, using gradient ascent algorithms as described in [17,22], it is possible to engineer the shape of $a(t)$ in Eq. (34), which optimizes the compensation against β and rf-inhomogeneity. We will address this problem in future work.

Acknowledgments

References

[1] S.J. Opella, NMR and membrane proteins, Nat. Struct. Biol. 4 (1997) 845–848 .
[2] R.G. Griffin, Dipolar recoupling in MAS spectra of biological solids, Nat. Struct. Biol. 5 (1998) 508–512.
[3] F. Castellani, B. van Rossum, A. Diehl, M. Schubert, K. Rehbein, H. Oschkinat, Structure of a protein determined by solid-state magic-angle-spinning NMR spectroscopy, Nature 420 (2002) 98–102.
[4] A.T. Petkova, Y. Ishii, J.J. Balbach, O.N. Antzutkin, R.D. Leapman, F. Deglaglio, R. Tycko, A structural model for alzheimer's β-amyloid fibrils based on experimental constraints from solid state NMR, Proc. Natl. Acad. Sci. USA 99 (2002) 16742–16747.
[5] C.P. Jaroniec, C.E. MacPhee, V.S. Baja, M.T. McMahon, C.M. Dobson, R.G. Griffin, High-resolution molecular structure of a peptide in an amyloid fibril determined by magic angle spinning NMR spectroscopy, Proc. Natl. Acad. Sci. USA 101 (2004) 711–716.
[6] J. Schaefer, R.A. McKay, E.O. Stejskal, Double-cross-polarization NMR of solids, J. Magn. Reson. 34 (1979) 443–447.
[7] M.H. Levitt, D. Suter, R.R. Ernst, Spin dynamics and thermodynamics in solid-state NMR cross polarization, J. Chem. Phys. 84 (8) (1986).
[8] D.M. Gregory, D.J. Mitchell, J.A. Stringer, S. Kiihne, J.C. Shiels, J. Callahan, M.A. Mehta, G.P. Drobny, Windowless dipolar recoupling: The detection of weak dipolar couplings between spin 1/2 nuclei with large chemical shift anisotropies, Chem. Phys. Lett. 246 (1995) 654–663.
[9] A. Detken, E.H. Hardy, M. Ernst, B.H. Meier, Simple and efficient decoupling in magic-angle spinning solid-state NMR: The XiX scheme, Chem. Phys. Lett. 356 (2002) 298–304.
[10] X. Wu, K.W. Zilm, Cross polarization with high-speed magic-angle spinning, J. Magn. Reson. A 104 (1993) 154.
[11] T. Gullion, J. Schaefer, Rotational-echo double-resonance NMR, J. Magn. Reson. 81 (1989) 196–200.
[12] D.P. Raleigh, M.H. Levitt, R.G. Griffin, Rotational resonance in solid state NMR, Chem. Phys. Lett. 146 (1988) 71–76.
[13] N.C. Nielsen, H. Bildsøe, H.J. Jakobsen, M.H. Levitt, Double-quantum homonuclear rotary resonance: Efficient dipolar recovery in magic-angle spinning nuclear magnetic resonance, J. Chem. Phys. 101 (1994) 1805–1812.
[14] Y.K. Lee, N.D. Kurur, M. Helmle, O.G. Johannessen, N.C. Nielsen, M.H. Levitt, Efficient dipolar recoupling in the NMR of rotating solids. A sevenfold symmetric radiofrequency pulse sequence, Chem. Phys. Lett. 242 (1995) 304–309.
[15] M. Hohwy, H.J. Jakobsen, M. Eden, M.H. Levitt, N.C. Nielsen, Broadband dipolar recoupling in the nuclear magnetic resonance of rotating solids: A compensated C7 pulse sequence, J. Chem. Phys. 108 (1998) 2686–2694.
[16] M.H. Levitt, Symmetry-based pulse sequences in magic-angle spinning solid-state NMR, in: Encyclopedia of NMR, Wiley, Chichester, 2002, pp. 165–196.
[17] N. Khaneja, C. Kehlet, S.J. Glaser, N.C. Nielsen, Composite dipolar recoupling: Anisotropy compensated coherence transfer in solid-state nuclear magnetic resonance, J. Chem. Phys. 124 (2006) 114503.
[18] M.H. Levitt, R. Freeman, Compensation for pulse imperfections in NMR spin-echo experiments, J. Magn. Reson. 43 (1981) 65–80.
[19] A.J. Shaka, R. Freeman, Composite pulses with dual compensation, J. Magn. Reson. 55 (1983) 487–493.
[20] M.H. Levitt, Composite Pulses, Prog. NMR Spectrosc. 18 (1986) 61–122.
[21] M.J. Duer, An Introduction to Solid-State NMR Spectroscopy, Blackwell Science Ltd, Oxford, 2004.
[22] N. Khaneja, T. Reiss, C. Kehlet, T. Schulte-Herbruggen, S.J. Glaser, Optimal control of coupled spin dynamics: Design of NMR pulse sequences by gradient ascent algorithms, J. Magn. Reson. 172 (2005) 296–305.
[23] M. Baldus, D.G. Geurts, S. Hediger, B.H. Meier, Efficient ^{15}N-^{13}C polarization transfer by adiabatic-passage Hartmann–Hahn cross polarization, J. Magn. Reson. A 118 (1996) 140–144.
[24] R. Verel, M. Baldus, M. Nijman, J.W.M. Vanus, B.H. Meier, Adiabatic homonuclear polarization transfer in magic-angle-spinning solid-state NMR, Chem. Phys. Lett. 280 (1997) 31–39.
[25] G. De Paëpe, M.J. Bayro, J. Lewandowski, R.G. Griffin, Broadband homonuclear correlation spectroscopy at high magnetic fields and MAS Frequencies, J. Am. Chem. Soc. 128 (2006) 1776–1777.
[26] G. De Paëpe, J. Lewandowski, R.G. Griffin, Spin dynamics in the modulation frame: Application to homonuclear recoupling in magic angle spinning solid-state NMR, J. Am. Chem. Soc. 128 (2008) 124503.